

Wavelet Analyses of Geomagnetic Data regarding Major Geomagnetic Disturbances

Laurentiu Asimopolos¹, Natalia-Silvia Asimopolos¹ and Adrian Aristide Asimopolos²

1. Geological Institute of Romania, Caransebes str. 1, 012271, Bucharest, Romania

2. Faculty of Transportation, University POLITEHNICA of Bucharest, Splaiul Independentei str. 313, 060042 Bucharest, Romania

Abstract: The purpose of this study was to analyze the associated spectrum of geomagnetic field, frequencies intensity and the time of occurrence. We calculated the variation of the correlation coefficients, with mobile windows of various sizes, for the recorded magnetic components at different latitudes and latitudes. The observatories we included in our study are USA (Surlari), HON (Honolulu), SBA (Scott Base), KAK (Kakioka), THY (Tihany), UPS (Uppsala), WNG (Wingst) and Yellowknife (YKC). We used the data of these observatories from International Real-time Magnetic Observatory Network (INTERMAGNET) for the geomagnetic storm from October 28-31, 2003. We have used for this purpose a series of filtering algorithms, spectral analysis and wavelet with different mother functions at different levels. In the paper, we show the Fourier and wavelet analysis of geomagnetic data recorded at different observatories regarding geomagnetic storms. Fourier analysis highlights predominant frequencies of magnetic field components. Wavelet analysis provides information about the frequency ranges of magnetic fields, which contain long time intervals for medium frequency information and short time intervals for highlight frequencies, details of the analyzed signals. Also, the wavelet analysis allows us to decompose geomagnetic signals in different waves. The analyses presented are significant for the studies of the geomagnetic storm. The data for the next days after the storm showed a mitigation of the perturbations and a transition to quiet days of the geomagnetic field.

Key words: Fourier spectral deconvolution, wavelet analyses, geomagnetic disturbances, geomagnetic observatories.

1. Introduction

A geomagnetic storm is a temporary disturbance of the Earth's magnetosphere caused by a disturbance in space weather. Associated with solar coronal mass ejections, coronal holes, or solar flares, a geomagnetic storm is caused by a solar wind shock wave which typically strikes the Earth's magnetic field 24 to 36 h after the event.

This only happens if the shock wave travels in a direction toward Earth. The solar wind pressure on the magnetosphere will increase or decrease dependence on the Sun's activity.

These solar wind pressure changes modify the electric currents in the ionosphere. Magnetic storms usually last 24 to 48 h, but some may last for many days.

These geomagnetic disturbances occur at the level of the entire planet, but with different intensities depending on the latitude of the location of the observatory in which we measure.

These geomagnetic storms or substorms may damage many technological or critical systems [1], depending on the intensity of the geomagnetic activity.

In Ref. [2], Kamide described recordings of geomagnetic storms in different geomagnetic observatories from point of view of amplitudes and energy flux of geomagnetic storm. Also, the analysis of geomagnetic storms is dealt with in many works from which we can recall the following: Refs. [3-7].

The wavelet analysis allows us to decompose a signal in different waves, called wavelets [8-11]. In the case of this paper, we refer to the magnetic field components. The wavelet methodology is described in detail in the signal processing documentation, such as

Corresponding author: Natalia-Silvia Asimopolos, MSc & PhD in Geophysics, MSc in Law, Researcher, research field: geophysics, gravity and geodesy.

Refs. [12-14]. In this paper, we refer to the data analyses of magnetic field components from Surlari National Geomagnetic Observatory and Refs. [15-17].

2. Methods

Wavelets allow local analysis of magnetic field components through variable frequency windows. Windows that contain longer time intervals allow us to extract low-frequency information, average ranges of different sizes lead to extraction of medium frequency information, and very narrow windows highlight the high frequencies or details of the analyzed signals. The wavelet functions describe the orthogonal bases in the $L^2(\mathbb{R})$ space, with signal approximation properties, while the orthonormal bases in the Fourier analysis are made up of sinusoidal waves.

Estimation of geomagnetic field disturbances is similar to the standard problem of estimating a signal disturbed by signal theory.

The term “noise” refers to any modification that changes the periodic or quasi-periodic characteristics of the original signal.

The model of the disturbed geomagnetic field is composed of periodic oscillations plus non-periodic oscillations given by the impact of solar wind on the terrestrial magnetosphere.

The purpose of wavelet analysis is to build orthonormal bases composed of wavelets that can reconstruct the geomagnetic signals recorded in the observatories.

In Fig. 1, we can see the different dimensions of time-frequency for the three transforms: wavelet transform, Fourier transform and STFT (Short Time Fourier Transform).

In these types of transformations, evaluation involves the calculation of a scalar product between the analysed signal (geomagnetic time series) and a set of signals that form a particular base in the vector space of the finite energy signals. Fourier representations use the basis of orthogonal vectors, while in the case of wavelets there is the possibility to use bases consisting of independent linear non-orthogonal vectors. Unlike the Fourier transform, which depends only on a single parameter, wavelet transform type depends on two parameters, a and b . As a result, the graphical representation of the spectrum is different, wavelet analysis bringing more information about geomagnetic pattern of each observatory with that specific condition. These advantages recommend multi-resolution analysis and wavelet analysis as very effective analysis tools for studying geomagnetic storms and space weather. The wavelet function is

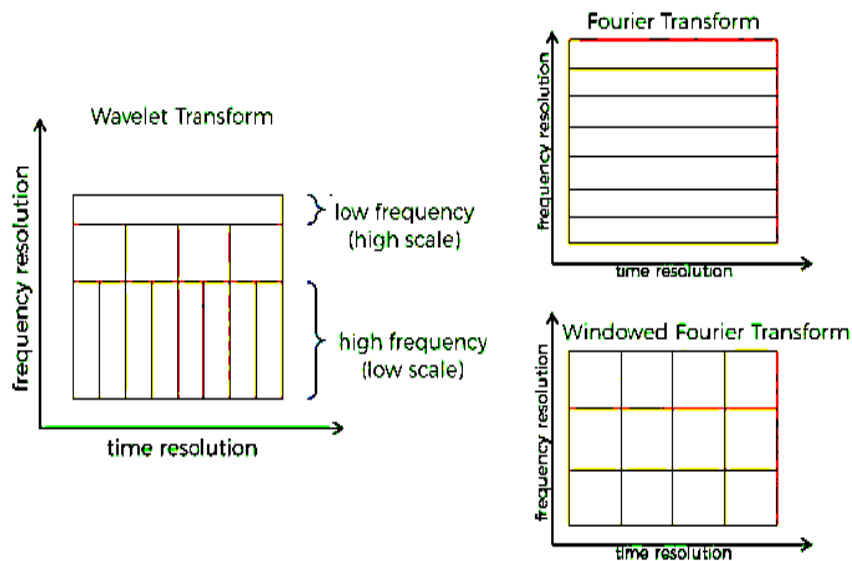


Fig. 1 Different time-frequency tile allocation of the three transforms: wavelet transform, Fourier transform, Windowed Fourier Transform (STFT).

designed to strike a balance between time domain (finite length) and frequency domain (finite bandwidth).

As we dilate and translate the mother wavelet, we can see very low frequency components at large scale (s) while very high frequency component can be located precisely at small scale (s).

The transition from STFT to wavelet was done by replacing a fixed-length analysis window, regardless of the frequency of the studied signal, with a set of variable duration analysis windows, so that at low frequencies we use long duration, and at high frequencies we use small durations.

To make Wavelet Continue Transform (CWT), a real or complex signal must satisfy the following two conditions:

$$\int_{-\infty}^{\infty} \psi(t) dt = 0 \quad , \quad \int_{-\infty}^{\infty} |\psi(t)|^2 dt < \infty$$

The first property, according to which the signal has a mean null value, suggests a possible oscillating aspect, while the second property, referring to the finite energy value, indicates that the signal concentrates most of the energy within a finite range of time.

The two conditions, together with a so-called admissibility condition (required to define the transformed wavelet inverse), are sufficient for a signal to “qualify” as a wavelet signal. In the literature, numerous such signals have been proposed, some of them with finite (thus, compact support) and others with infinite duration, but with concentrated energy within a finite timeframe.

3. Results

In this paper we used spectral analysis and wavelet tools from signal processing in MATLAB.

We used for Fourier analysis the MATLAB code (MATLAB software 2011):

```
load table.txt; X1= table (:,1); X2= table (:,2); X3=
table (:,3); N=length(X1); t=1:1:N; fe=1/N; x=X1';
Xt=fft(x); Xm=abs(Xt); X=Xm(1,1:N/2+1)/(N/2);
```

```
f=[0:N/2]*fe; subplot(211); plot(t,x); grid;
xlabel('t[min]'); ylabel('x(t)[ ]'); title(' '); subplot(212);
stem(f,X); xlabel('f[0.5Hz]'); ylabel('X(f)'); grid;
title('')
```

For wavelet analysis we used function Daubechies db1, level 5, the same wavelet as Haar, with following code:

```
load table.txt; SX=table(:,1); signal = SX; lev =
5; wname = 'db1'; nbc col = 64; [c,l]
=wavedec(signal,lev,wname); len = length(signal); cfd
= zeros(lev,len); for k = 1:lev; d = detcoef(c,l,k); d =
d(:); d = d(ones(1,2^k),:); cfd(k,:) = wkeep1(d(:),len);
end cfd = cfd(:); I = find(abs(cfd)<sqrt(eps)); cfd(I)
= zeros(size(I)); cfd = reshape(cfd,lev,len); cfd =
wcodemat(cfd,nbc col,'row'); h211 = subplot(2,1,1);
h211.XTick = []; plot(signal,'r'); title('Analyzed
signal. '); ax = gca; ax.XLim = [1 length(signal)];
subplot(2,1,2); colormap(cool(128)); image(cfd); tics
= 1:lev; labs = int2str(tics); ax = gca;
ax.YTickLabelMode = 'manual'; ax.YDir = 'normal';
ax.Box = 'On'; ax.YTick = tics; ax.YTickLabel = labs;
title('Discrete Transform, absolute coefficients. ');
ylabel('Level'); figure; [cfs,f] =
cwt(signal,1,'waveletparameters',[3 3.1]); hp =
pcolor(1:length(signal),f,abs(cfs)); hp.EdgeColor =
'none'; set(gca,'YScale','log'); xlabel('Sample');
ylabel('log10(f));
```

For wavelet coherences:

```
load table1.txt; load table2.txt; X=table1(:,1);
Y=table2(:,1); wcoherence(X,Y)
```

These types of analyses resulted in a precise localization of the times when the high frequency components represented by the pulsations were present, as well as the value of the low frequency components represented by the periodic oscillations of 8 h, 12 h and 24 h.

Fig. 2 shows the North geomagnetic field on October 28, 2003 (biggest geomagnetic storm in the last twenty years) at Surlari Observatory and spectral analysis and in Fig. 3 is its derivative and spectral analysis.

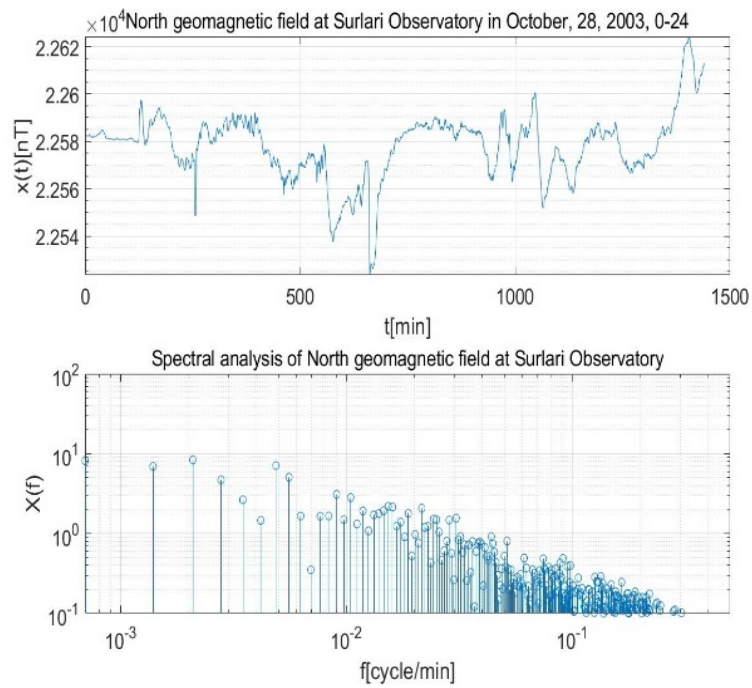


Fig. 2 North geomagnetic field on Surlari Observatory, on October 28th, 2003, 0:24, minute mean, and spectral analyses.

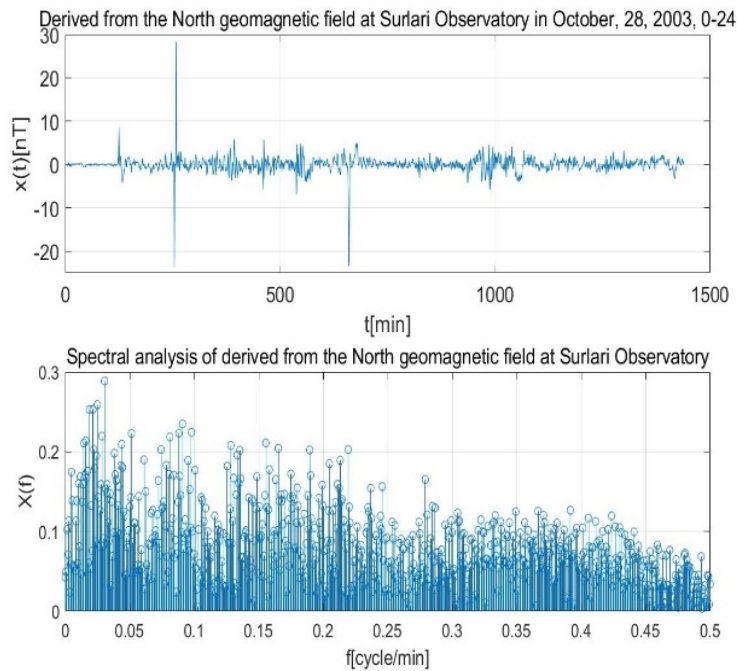


Fig. 3 Derived from the North geomagnetic field on Surlari Observatory, on October 28th, 2003 and spectral analyses.

Figs. 4-9 show the wavelet power spectra themselves, an important advantage of wavelet analysis over spectral analysis. On the horizontal axis we have the

time dimension. The vertical axis gives us the periods. The power is given by the colour. The colour code indicates ranges of power from blue to yellow.

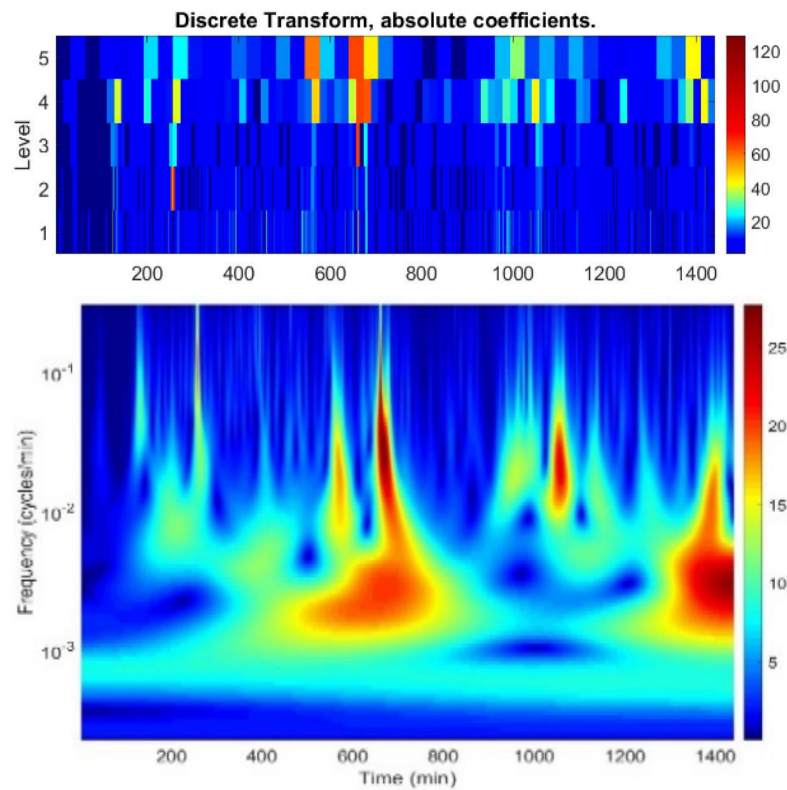


Fig. 4 Absolute coefficients, function db1, level 5 and wavelet image with frequency, time and amplitude, for North geomagnetic field.

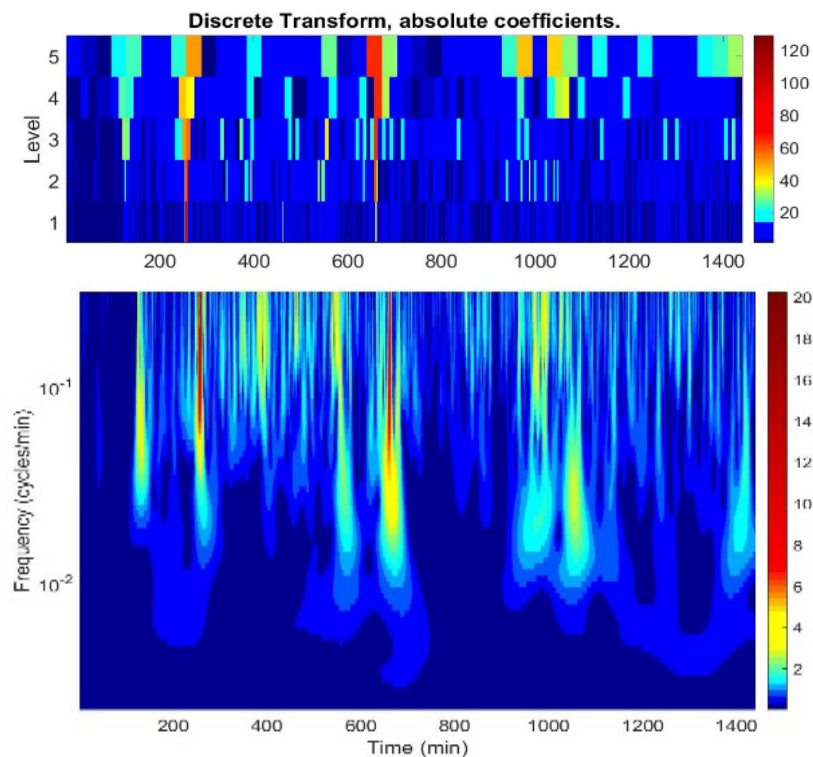


Fig. 5 Absolute coefficients, function db1, level 5 and wavelet image with frequency, time and amplitude for derivation of North geomagnetic field.

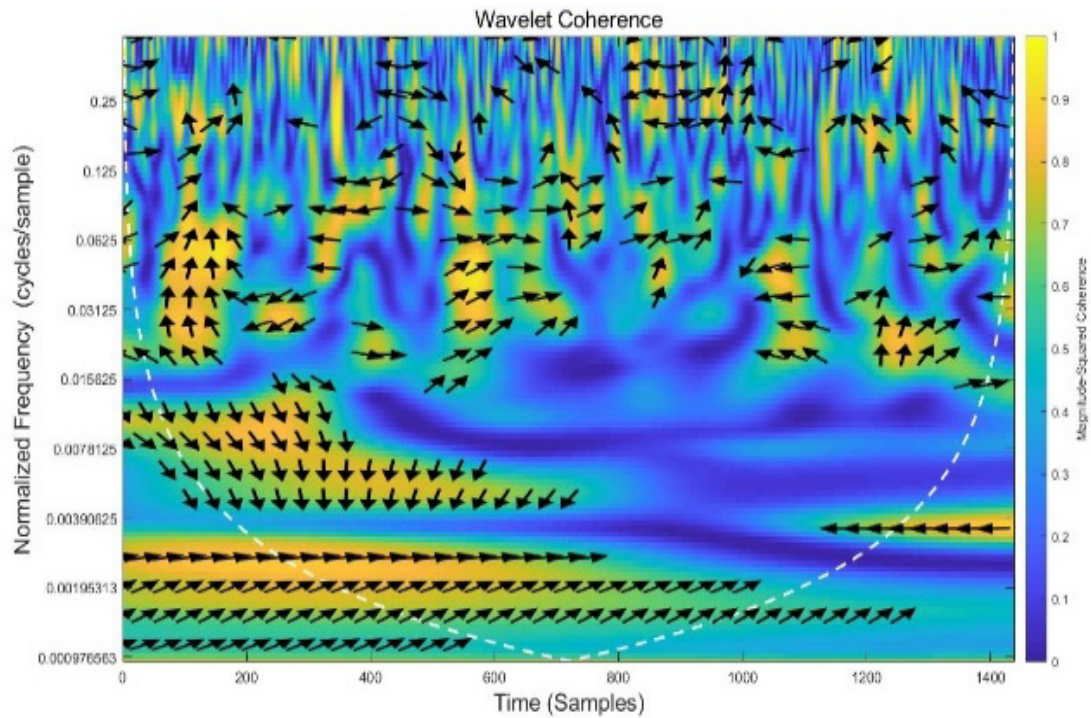


Fig. 6 Wavelet coherences between minute means of North components of the geomagnetic field, on October 28th, 2003, from Surlari Observatory and HON (Honolulu) Observatory.

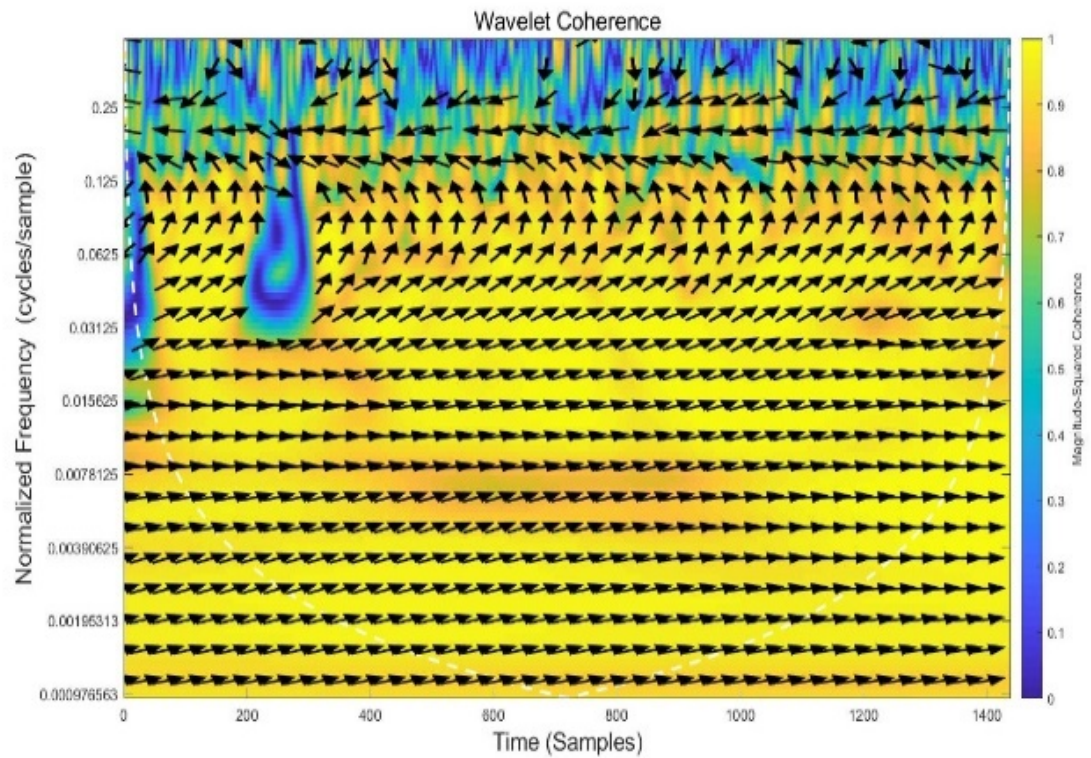


Fig. 7 Wavelet coherences between minute means of North components of the geomagnetic field, on October 28th, 2003, from Surlari Observatory and THY (Tihany) Observatory.

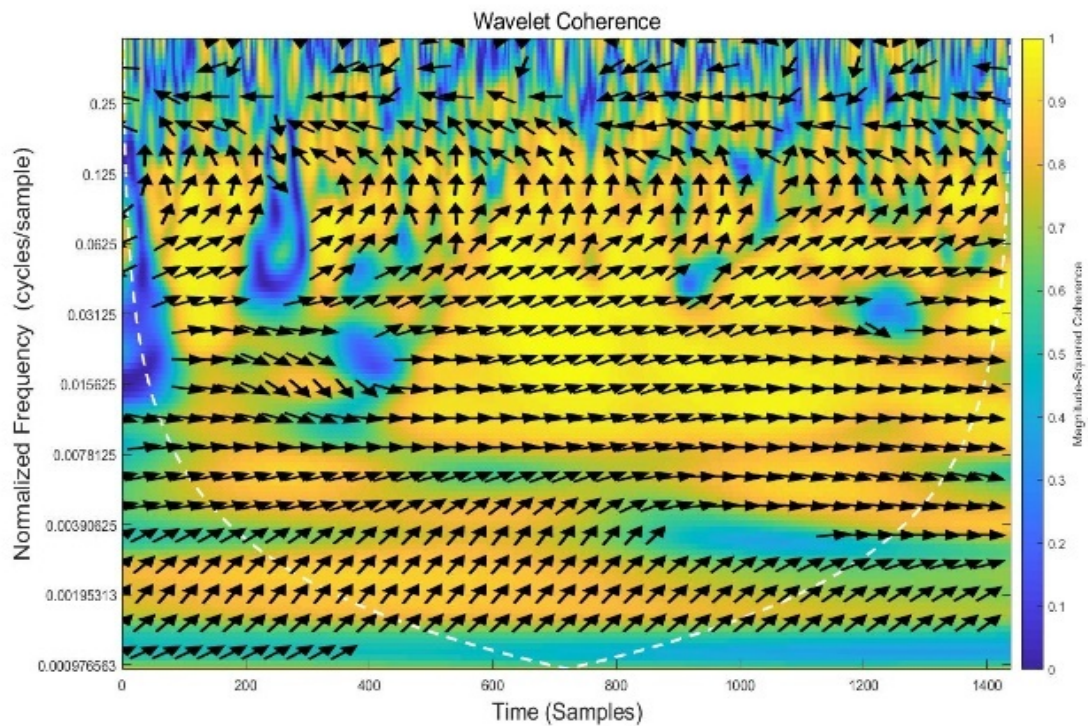


Fig. 8 Wavelet coherences between minute means of North components of the geomagnetic field, on October 28th, 2003, from Surlari Observatory and WNG (Wingst) Observatory.

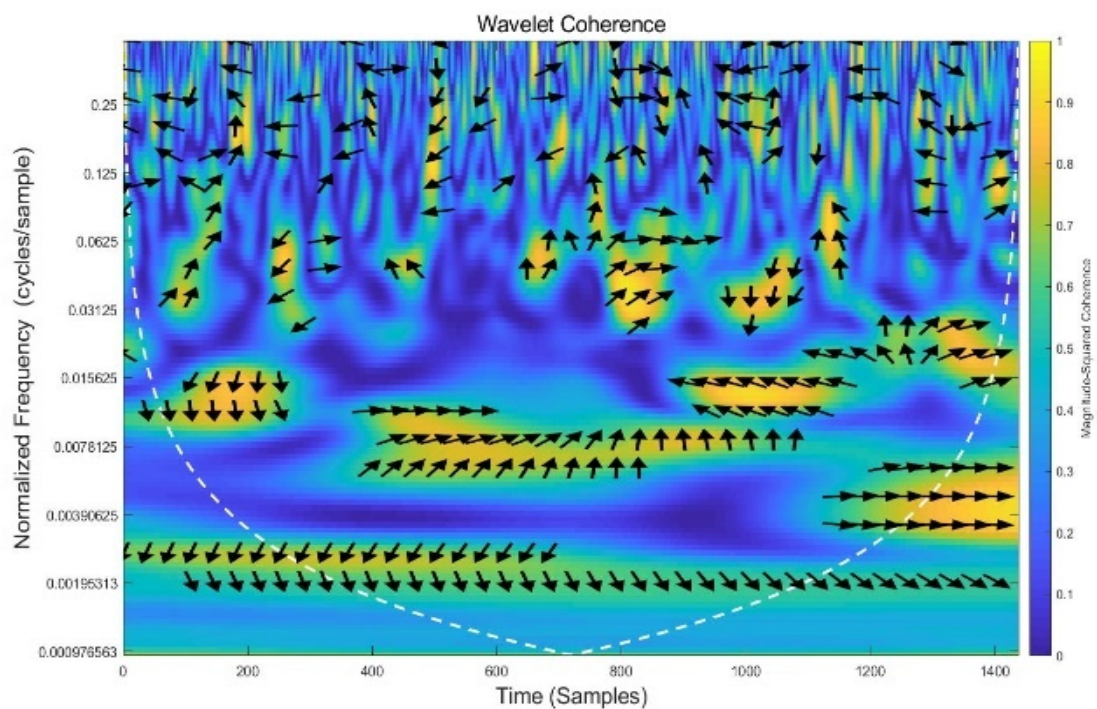


Fig. 9 Wavelet coherences between minute means of North components of the geomagnetic field, on October 28th, 2003, from Surlari Observatory and YKC (Yellowknife) Observatory.

Figs. 6-9 are show the wavelet coherence between geomagnetic field recorded at different observatories during the geomagnetic storm and display the result. The sampling rate was 1 min and a time-frequency plot of the wavelet coherence was obtained, used to indicate the relative lag between coherent components [13]. The arrows are oriented in the direction of the phase difference between the two signals.

These types of analyses resulted in a precise localization of the times when the high frequency components represented by the pulsations were present, as well as the value of the low frequency components represented by the periodic oscillations of 8 h, 12 h and 24 h. The maximum period of magnetic disturbance was manifested by a decrease or even a lack of periodic oscillations. Another advantage of wavelet analysis refers to the intervals in which sudden variations in the amplitude of the analysed geomagnetic signal are present and unaltered.

4. Conclusion

While the Fourier transform cannot show which of the harmonic components is present at a time in the geomagnetic data series, wavelet analysis gives us information in the form of a three-dimensional graph (time, frequency, amplitude) or a two-dimensional shape, when the amplitude is encoded by colour intensity levels.

A first step in the wavelet analysis is STFT, applied successively with different narrow windows, for the best accuracy of time location. Increasing the window improves the resolution in frequency but decreases the resolution in time.

Although wavelet analysis provides additional information in comparison with Fourier analysis, it should be viewed under the Heisenberg principle of uncertainty, which states that the product between time and frequency of a signal is limited to a non-zero value.

One of the advantages of wavelet analysis compared to Fourier analysis is the flexibility in

choosing the mother function.

The wavelet transform is one of the ways of representing the signals in the multi-resolution analysis where the analysed geomagnetic signal is described by a sequence of approximations that contain more and more information.

Each level of approximation contains on the one hand all the information available at the previous level plus an additional detail component.

Acknowledgement

Authors address their thanks to the Romanian Ministry of Education and Research for financing the projects “The realization of 3D geological/geophysical models for the characterization of some areas of economic and scientific interest in Romania”, with Contract No. 49N/2019 and “Institutional capacities and services for research, monitoring and forecasting of risks in extra-atmospheric space”, acronym SAFESPACE, project Nr.16PCCDI/2018, within PNCDIII. Also, we are grateful for the many and significant contributions and comments provided by our colleagues from geomagnetic observatories and for data used from INTERMAGNET.

References

- [1] Gannon, J. L., Swidinsky, A., and Xu, Z. 2019. “Geomagnetically Induced Currents from the Sun to the Power Grid.” In *Geophysical Monograph Series*. Hoboken, NJ: John Wiley & Sons, Inc. ISBN: 9781119434344.
- [2] Kamide, Y. 2006. *Geomagnetic Storm*. Solar Terrestrial Environment Laboratory Nagoya University, Japan.
- [3] Asimopolos, N. S., and Asimopolos, L. 2018. “Study on the High-Intensity Geomagnetic Storm from March 2015, Based on Terrestrial and Satellite Data.” *Micro and Nano Tehnologies & Space Tehnologies & Planetary Science* 18: 593-600. doi: 10.5593/sgem2018/6.1.
- [4] Asimopolos, L., Săndulescu, A. M., Asimopolos, N. S., and Niculici, E. 2012. “Analysis of Data from Surlari National Geomagnetic Observatory.” Editura Ars Docendi a Universitatii din Bucuresti, pp. 1-96. ISBN: 978-973-558-588-4.
- [5] Asimopolos, L., Niculici, E., Săndulescu, A. M., and Asimopolos, N. S. 2011. “Comparisons of Geomagnetic

- Data Measured in Romania with the Data of International Geomagnetic Reference Field 11 (IGRF 11).” *Surveying Geology & Mining Ecology Management* 2: 25-32. doi: 10.5593/sgem2011.
- [6] Benoit, S. L. 2012. *INTERMAGNET Technical Reference Manual*, Version 4.6. UK: Murchison House West Mains Road Edinburgh EH9 3LA, pp. 1-100.
- [7] Gebbins, D., and Herrero-Bervera, E. 2006. *Encyclopedia of Geomagnetism and Paleomagnetism*. London: Springer, pp. 311-60. ISBN: 9781402039928.
- [8] Box, G. E. P., Jenkins, G. M., and Reinsel, G. C.. 1994. *Time Series Analysis: Forecasting and Control*, 3rd ed. Englewood Cliffs, NJ: Prentice Hall.
- [9] Chatfield, C. 1989. *The Analysis of Time Series: An Introduction*, 4th ed. London: Chapman and Hall, pp. 1-241.
- [10] Liu, C. L. 2010. “A Tutorial of the Wavelet Transform.” <http://disp.ee.ntu.edu.tw/tutorial/WaveletTutorial.pdf>.
- [11] Daubechies, I. 1990. “The Wavelet Transforms Time-Frequency Localization and Signal Analysis.” *IEEE Trans. Inform. Theory* 36: 961-1004. doi: 10.1109/18.57199.
- [12] MATLAB Software. 2011. The Language of Technical Computing. The MathWorks. www.mathworks.com/help/matlab/.
- [13] <https://www.mathworks.com>.
- [14] Torrence, C., and Compo, G. P. 1998. “A Practical Guide to Wavelet Analysis.” *Bull. Amer. Meteor. Soc.* 79 (1): 61-78. doi.org/10.1175/1520-0477(1998)079<0061:APGTWA>2.0.CO;2.
- [15] <http://www.intermagnet.org>.
- [16] <http://www.noaa.gov>.
- [17] <https://www.spaceweatherlive.com>.